Overexpression of ubiquitin-conjugating enzyme E2 L3 in hepatocellular carcinoma potentiates apoptosis evasion by inhibiting the GSK3β/p65 pathway

Na-Na Tao, Zhen-Zhen Zhang, Ji-Hua Ren, Juan Zhang, Yu-Jiao Zhou, Vincent Kam Wai Wong, Betty Yuen Kwan Law, Sheng-Tao Cheng, Hong-Zhong Zhou, Wei-Xian Chen, Hong-Mei Xu, Juan Chen

PII: S0304-3835(20)30161-0

DOI: https://doi.org/10.1016/j.canlet.2020.03.028

Reference: CAN 114752

To appear in: *Cancer Letters*

Received Date: 21 November 2019

Revised Date: 19 March 2020

Accepted Date: 26 March 2020

Please cite this article as: N.-N. Tao, Z.-Z. Zhang, J.-H. Ren, J. Zhang, Y.-J. Zhou, V.K. Wai Wong, B.Y. Kwan Law, S.-T. Cheng, H.-Z. Zhou, W.-X. Chen, H.-M. Xu, J. Chen, Overexpression of ubiquitin-conjugating enzyme E2 L3 in hepatocellular carcinoma potentiates apoptosis evasion by inhibiting the GSK3β/p65 pathway, *Cancer Letters*, https://doi.org/10.1016/j.canlet.2020.03.028.

Abstract

UBE2L3 is a ubiquitin-conjugating protein belonging to the E2 family that consists of 153 amino acid residues. In this study, we found that UBE2L3 was generally upregulated in clinical HCC samples compared to non-tumour samples and that there was a strong association between high UBE2L3 expression and tumour size, clinical grade and prognosis in HCC patients. UBE2L3 depletion inhibited the proliferation and induced the apoptosis of HCC cells. At the molecular level, we observed that UBE2L3 depletion enhanced the protein stability of GSK3β, thus promoting the expression and activation of GSK3β. Subsequently, activated GSK3β phosphorylated p65 and promoted its nuclear translocation to increase the expression of target genes, including PUMA, Bax, Bim, Bad, and Bid. *In vivo*, knockout of UBE2L3 in HCC cells inhibited tumour growth in orthotopic liver injection nude mouse models. Moreover, inhibition of p65 or GSK3β significantly restored the effects induced by UBE2L3 knockout in HCC. Together, this study reveals the stimulatory effect of UBE2L3 on HCC cell proliferation, suggesting that UBE2L3 may be an important pro-tumorigenic factor in liver carcinogenesis and a potential therapeutic target of HCC.

Overexpression of ubiquitin-conjugating enzyme E2 L3 in hepatocellular carcinoma potentiates apoptosis evasion by inhibiting the GSK3β/p65 pathway

Na-Na Tao[1,2#], Zhen-Zhen Zhang[1#], Ji-Hua Ren[3#], Juan Zhang[2], Yu-Jiao Zhou[3,] Vincent Kam Wai Wong[4], Betty Yuen Kwan Law[4], Sheng-Tao Cheng[3], Hong-Zhong Zhou[3], Wei-Xian Chen[5], Hong-Mei Xu[1*], Juan Chen[1*]

[1] Department of infectious disease; Ministry of Education Key Laboratory of Child Development and Disorders; National Clinical Research Center for Child Health and Disorders (Chongqing); China International Science and Technology Cooperation base of Child development and Critical Disorders; Children's Hospital of Chongqing Medical University, Chongqing, China; [2] Department of Clinical Laboratory, Chongqing Traditional Chinese Medicine Hospital, Chongqing, China;[3] The Key Laboratory of Molecular Biology of Infectious Diseases designated by the Chinese Ministry of Education, Chongqing Medical University, Chongqing, China; [4] State Key Laboratory of Quality Research in Chinese Medicine, Macau University of Science and Technology, Macau, China; [5]Department of Clinical Laboratory, The Second Affiliated Hospital of Chongqing Medical University, Chongqing, China;

[#]These authors contributed equally to this work.

Running title: The role of UBE2L3 in Hepatocellular Carcinoma

Key words: Hepatocellular Carcinoma; UBE2L3; Apoptosis; GSK3β

***Corresponding Authors:**

Contact Information:

Juan Chen, Prof., Room 617, College of Life Sciences Building, 1 YiXueYuan Road, YuZhong District, Chongqing, 400016, China, Telephone Number: +86-23-68486780, Fax: +86-23-68486780, Email: chenjuan2014@cqmu.edu.cn.

Hong-Mei Xu, Prof., No 136, ZhongShan Er Road, Children's Hospital of ChongQing Medical University, YuZhong Distric, ChongQing, 400014, China, Telephone Number: +86-23-63624014, Fax: +86-23-63624014, Email: xuhongm0095@cqmu.edu.cn

Conflict of Interest Disclosure: The authors disclose no potential conflicts of interest.

Financial Support: National Natural Science Foundation of China (81861168035, 81871656 and 81922011, JC), Chongqing Natural Science Foundation (cstc2018jcyjAX0114, JC, cstc2019jcyj-msxmX0041, NN T and cstc2018jcyjAX0485, JH R) and Creative Research Group of CQ University (CXQT19016, JC).

Abstract

UBE2L3 is a ubiquitin-conjugating protein belonging to the E2 family that consists of 153 amino acid residues. In this study, we found that UBE2L3 was generally upregulated in clinical HCC samples compared to non-tumour samples and that there was a strong association between high UBE2L3 expression and tumour size, clinical grade and prognosis in HCC patients. UBE2L3 depletion inhibited the proliferation and induced the apoptosis of HCC cells. At the molecular level, we observed that UBE2L3 depletion enhanced the protein stability of GSK3β, thus promoting the expression and activation of GSK3β. Subsequently, activated GSK3β phosphorylated p65 and promoted its nuclear translocation to increase the expression of target genes, including PUMA, Bax, Bim, Bad, and Bid. *In vivo*, knockout of UBE2L3 in HCC cells inhibited tumour growth in orthotopic liver injection nude mouse models. Moreover, inhibition of p65 or GSK3β significantly restored the effects induced by UBE2L3 knockout in HCC. Together, this study reveals the stimulatory effect of UBE2L3 on HCC cell proliferation, suggesting that UBE2L3 may be an important pro-tumorigenic factor in liver carcinogenesis and a potential therapeutic target of HCC.

1. Introduction

Hepatocellular carcinoma (HCC) is one of the most common malignancies in the world. In 2018, an estimated 841,000 new liver cancer cases and 782,000 liver cancer-related deaths occurred worldwide[1]. In general, Eastern and Southeastern Asia and parts of Africa have the highest morbidity and mortality associated with HCC[1]. Although many measures have been used in preventing and treating this disease, liver cancer is still a rapidly progressing malignancy with a poor prognosis. Currently, how cancer cells evade death signals is not fully understood; thus, it is urgent to clarify the complicated molecular mechanisms of HCC development and gain insight into new therapeutic targets for HCC treatment.

Post-translational modification (PTM) of proteins, such as ubiquitination, phosphorylation, acetylation and glycosylation, is an important way to preserve the biological functions of proteins in eukaryotes. Ubiquitin (Ub) is a highly conserved 8.5 kDa protein first found by Goldstein et al. in 1975 [2]. Ubiquitination plays a central role in many cellular processes, including cell cycle, proliferation, apoptosis, differentiation, DNA replication and DNA repair [3-7]. The dynamic balance between the synthesis and degradation of proteins is essential to maintain cellular homeostasis [8]. The ubiquitin-proteasome system (UPS) is a major pathway for protein degradation and is involved in more than 80% of intracellular protein degradation. The UPS contains six parts, including Ub and a ubiquitin-activating enzyme (E1), a ubiquitin-conjugating protein (E2), a ubiquitin-protein ligase enzyme (E3), the 26S proteasome and a deubiquitinase (DUB) [9]. First, E1 activates Ub in an ATP-dependent manner and ligates Ub to E2; then, the activated Ub is conjugated to the target protein via E3. Finally, the target protein will be degraded by the 26S proteasome [10].

UBE2L3, a member of the E2s, encodes 153 amino acid residues. In recent years, emerging evidence has confirmed that UBE2L3 plays important roles in many cellular functions by regulating protein stability. UBE2L3 has been demonstrated to promote

ubiquitination and degradation of p53, which leads to reduced apoptosis in HeLa cells [11, 12]. Moreover, depletion of UBE2L3 has been reported to stabilize tumour suppressor signal p53-binding protein 1 (53BP1), resulting in reduced homologous recombination for double-strand break repair [13]. Additionally, UBE2L3 has also been found to induce the degradation of MAP1B-LC1 by ubiquitination and finally affect the release of neurotransmitters [14]**.** Recently, the functions of UBE2L3 in some cancer cells were investigated. UBE2L3 was reported to promote the ubiquitination and degradation of p27kip1 in non-small-cell lung cancer (NSCLC), and further investigation showed that high levels of UBE2L3 and low levels of p27kip1 were correlated with poor prognosis of NSCLC[15]. Another study concluded that UBE2L3 fused to KRAS might drive metastatic progression in a rare subset of prostate cancers[16]. However, the function of UBE2L3 in HCC remains unclear.

In this study, we demonstrate that the expression of UBE2L3 is frequently upregulated in clinical HCC samples. In addition, we discover that UBE2L3 could play a pro-oncogenic role in HCC cells via the GSK3β/p65 signalling pathway.

2. Materials and Methods

2.1 Clinical samples

Human HCC tissues and adjacent non-tumorous liver tissues were collected from the First Affiliated Hospital of Chongqing Medical University. Written informed consent was obtained from each patient. The study protocol was approved by the Clinical Research Ethics Committee of Chongqing Medical University.

2.2 Cell culture, transfection and reagents

The hepatoma cell line Huh-7 was obtained from HSRRB (the Health Science Research Resource Bank), and the hepatoma cell line PLC/PRF/5 was obtained from ATCC (American Type Culture Collection). Cells were maintained in Dulbecco's modified Eagle's medium (DMEM, HyClone, UT, USA) supplemented with 10% foetal bovine serum (Gibco, NY, USA) and 1% penicillin/streptomycin (Thermo Fisher Scientific, MA, USA) and cultivated in a humidified incubator containing 5% CO_2 at 37°C. Transfection was performed with Lipofectamine® 3000 Transfection Reagent (Invitrogen, MA, USA). GSK3β inhibitor 1-azakenpaullone (S7193), p65 inhibitor JSH-23 (S7351) and proteasome inhibitor MG132 (S2619) were purchased from Selleckchem (TX, USA). The protein synthesis inhibitor cycloheximide (CHX, 97064-722) was commercially obtained from AMRESCO (OH, USA).

2.3 Plasmids and antibodies

Short hairpin RNA targeting UBE2L3 (shUBE2L3-1 and shUBE2L3-2) and nontargeting shRNA (shCont) were purchased from Shanghai Genechem Company Limited. The UBE2L3 overexpression vector was constructed by subcloning its coding sequence into the pcDNA3.1 vector with BamHI and XhoI restriction enzymes. To construct the pcDNA3.1-UBE2L3^{C86S} expression vector, we replaced cysteine 86 with serine by single base substitution. Anti-UBE2L3 (#8721), anti-p65 (#8242), anti-p-p65 (#3033), anti-PUMA (#12450), anti-GSK3β (#12456, #9832), anti-p-GSK3β (#5558), anti-Ub (#3936), anti-PARP (#9542), anti-cleaved PARP (#9542), anti-caspase-3 (#9662), anti-cleaved caspase-3 (#9662), anti-caspase-9

(#9502), anti-cleaved caspase-9 (#9502) and anti-histone H3 (#3638) were purchased from Cell Signaling Technology (CST, MA, USA). Anti-GAPDH (sc-365062), anti-β-actin (sc-1616) and anti-IgG (sc-66931) were purchased from Santa Cruz Biotechnology (CA, USA).

2.4 Quantitative real-time PCR (qPCR)

Total RNA was isolated with TRIzol reagent (Invitrogen, USA) and reverse transcribed into cDNA by using an iScript® cDNA Synthesis Kit (Bio-Rad, CA, USA). Quantitative real-time PCR was carried out by using the IQTM 5 Multicolor Real-Time PCR Detection system (Bio-Rad) and FastStart Universal SYBR Green Master Mix (Roche, Basel, Switzerland). The level of β-actin mRNA was used for data normalization. Values of target genes were calculated by using the $2^{-\Delta\Delta Ct}$ method. All qPCR experiments were performed in triplicate.

2.5 Western blotting analysis

Total proteins were lysed using RIPA lysis buffer containing EDTA-free protease inhibitor cocktail tablets (Roche, Basel, Switzerland). Equivalent aliquots of total protein lysates, which were determined by BCA Protein Assay Kit (Thermo), were separated by SDS-PAGE and transferred to PVDF membranes (GE Healthcare, Freiburg, Germany). Then, the membrane was blocked with 5% nonfat milk and incubated with the indicated primary antibodies and horseradish peroxidase-conjugated secondary antibodies. Detection was performed with Immobilon Western Chemiluminescent HRP Substrate (Millipore, MA, USA).

2.6 Immunohistochemistry

Immunohistochemistry was performed with paraffin-embedded sections. After xylene deparaffinization and rehydration, antigen retrieval was achieved by microwaving the sections in 10 mM sodium citrate buffer (pH 6.0). After quenching the endogenous peroxidase activity with hydrogen peroxide, the sections were incubated with goat serum for 30 min at room temperature and subsequently incubated with primary antibodies overnight at 4°C. Signals were detected by ABC

and DAB kits (Vector Laboratories, CA, USA). Counterstaining was performed using haematoxylin. Staining intensity and the percentage of positive cells were scored by two independent pathologists.

2.7 Cell proliferation assay

Cells were seeded into 6-well plates. The number of viable cells was observed at days 3, 4, and 5 after transfection by trypan blue exclusion assay. Each well was assessed in triplicate. All trypan blue exclusion assays were repeated three times.

2.8 Colony formation assay and soft agar assay

For the colony formation assay, briefly, 2×10^3 cells per well were seeded into 6-well plates and cultured for 14 days. The colonies were fixed with methanol and stained with 0.5% crystal violet. With respect to the soft agar assay, 1×10^3 cells were cultured in an upper layer of 0.35% low melting-point agarose, followed by a sublayer of 0.6% low melting-point agarose. Cells were maintained for 21 days, and 0.5 ml of fresh culture medium was added every 3 days. The colonies were stained with 0.005% crystal violet. All colony formation assays and soft agar assays were repeated three times.

2.9 Flow cytometric analysis for apoptosis

Cells were labelled with annexin V-FITC and propidium iodide (PI) and analysed by flow cytometry. All flow cytometric analyses were repeated three times.

2.10 Immunofluorescence

Cells seeded on coverslips were transfected with shCont and shUBE2L3. Seventy-two hours after transfection, cells were fixed with 4% paraformaldehyde and permeabilized with 0.1% Triton X-100 at room temperature. The primary antibody against p65 was used overnight at 4°C with a 1:100 dilution after blocking with 1% BSA in PBS for 45 min. p65 antibody-antigen complexes were visualized by using Alexa Fluor 488® anti-rabbit IgG. Cells were counterstained with DAPI to label the nuclei. Immunofluorescence images were visualized by a TCS-SP5X microscope (Leica, UK).

2.11 Extraction of cytoplasmic and nuclear proteins

Cytoplasmic and nuclear proteins were extracted by using NE-PER® Nuclear and Cytoplasmic Extraction Reagents (78833) (Thermo Fisher Scientific) according to the manufacturer's instructions.

2.12 Dual-luciferase reporter assay

NF-κB firefly luciferase reporter vectors were co-transfected with the indicated plasmids. The Renilla luciferase expression vector was co-transfected for normalization. Cells were harvested at 40 h post-transfection, and luciferase activities were determined with the Dual-Luciferase Report Assay System (Promega, WI, USA) according to the manufacturer's instructions in a GloMax microplate luminometer (Promega). Normalization of NF-κB firefly luciferase values in each well was carried out according to Renilla luciferase activity. All dual-luciferase reporter assays were repeated three times.

2.13 Co-immunoprecipitation assay

Cells were lysed, and then the protein concentrations were determined by the method mentioned above. Cellular extracts were precleared with Protein G Magnetic Beads (Millipore) for 60 min at 4 °C and incubated overnight at 4 °C with appropriate primary antibodies and IgG. Protein G magnetic beads were then added to capture the immunoprecipitates for 120 min at room temperature. Captured immunoprecipitates were subjected to SDS-PAGE for immunoblotting analysis with the indicated antibodies.

2.14 Mice model

Ten six-week-old male BALB/c nude mice were randomly divided into 2 groups. Huh-7 cells were resuspended in 200 μL DMEM/Matrigel (1:1 mixture) and subcutaneously injected into nude mice (n = 5 per group) to generate a mouse model. Tumour size was monitored by bidimensional measurements using a calliper. Four weeks after inoculation, mice were sacrificed, and the tumours were removed for further studies. In addition, Huh-7 cells were resuspended in 40 μl DMEM/Matrigel

(1:1 mixture) and injected into the left lobe of liver of nude mice (n = 5 per group) to prepare an orthotopic liver cancer model. All animal experiments were performed according to the protocol approved by the Chongqing Medical University Animal Care Committee and satisfied the NIH guidelines.

2.15 Statistical analyses

Data were analysed using SPSS 19.0 software (IBM Corporation, USA). Survival curves were estimated using the Kaplan-Meier method. Differences between the survival curves were assessed by the log-rank test. Differences between groups were determined by Student's t test, the Mann-Whitney U test or one-way ANOVA. Correlations between UBE2L3 and individual clinicopathologic parameters were evaluated using the nonparametric chi-square test. A value of $P < 0.05$ was considered significant.

3. Results

3.1 UBE2L3 is upregulated in HCC tissues and correlates with the survival of HCC patients

To demonstrate the role of UBE2L3 in HCC, we evaluated the expression of UBE2L3 in two independent datasets (GSE14520, GSE25097) from NCBI's Gene Expression Omnibus (GEO). As shown in Figure 1A, UBE2L3 mRNA levels were significantly upregulated in HCC tissues. Importantly, Kaplan-Meier analysis showed that patients with higher levels of UBE2L3 had a significantly shorter overall survival than patients with lower levels of UBE2L3 (median OS time, 37.75 and 70.01 months, respectively; difference=32.26 months; P=0.0008), and the same trend was observed for disease-free survival (median DFS time, 14.22 and 25.49 months; difference=11.27 months; P=0.0026) (Figure 1B).

To verify the correlation between UBE2L3 expression level and HCC, we first detected UBE2L3 mRNA and protein levels in 90 HCC tissues and paired adjacent non-tumour liver tissues by qPCR and western blotting analysis, respectively. According to the results, UBE2L3 mRNA and protein levels were upregulated in HCC tissues (Figure 1C). UBE2L3 protein levels in 66 (66/90, 73.3%) HCC tissues were higher than those in adjacent HCC-free liver tissues (Figure 1D). In addition, differential expression of UBE2L3 was observed by immunohistochemistry (IHC). As shown in Figure 1E, UBE2L3 immunoreactivity was separately graded as weak, moderate, and strong. Furthermore, our results showed that a high UBE2L3 protein level was significantly associated with tumour size and clinical grade (Table 1). Conclusively, these results indicate that the expression of UBE2L3 is upregulated in HCC tissues and is closely related to the poor prognosis of HCC patients.

3.2 UBE2L3 deficiency inhibits proliferation and tumorigenesis of HCC in vitro and in vivo

As a high UBE2L3 protein level was significantly associated with tumour size, we speculated that UBE2L3 might play an important role in HCC development. To

investigate the effect of UBE2L3 on HCC cell proliferation, we suppressed the expression of UBE2L3 via shRNA-mediated knockdown or CRISPR/Cas9-mediated knockout. Trypan blue exclusion assay revealed that UBE2L3 knockdown/knockout significantly reduced the proliferation ability of HCC cells (Figure 2A). Furthermore, colony formation assays and soft agar assays showed that UBE2L3 knockdown/knockout inhibited HCC cell colony formation ability and anchorage-independent growth ability, respectively (Supplementary Figure 1). Flow cytometry also showed that UBE2L3 knockdown/knockout significantly increased the apoptotic rate of HCC cells (Figure 2B). Additionally, western blotting analysis indicated that the levels of several apoptotic markers, including cleaved PARP, cleaved caspase-3 and cleaved caspase-9, were increased in UBE2L3 knockdown/knockout cells compared to control cells (Figure 2C).

On the other hand, according to xenograft nude mouse models, we found that the tumour growth rate in the UBE2L3 knockout group was slower than that in the parental control group (Figure 2D). Similarly, tumours in the UBE2L3 knockout group had lower volumes and weights than those in the parental control group (Figure 2E-F). Taken together, these data demonstrate that UBE2L3 deficiency suppresses HCC cell proliferation, promotes apoptosis, and inhibits HCC tumorigenesis.

3.3 UBE2L3 overexpression promotes cell proliferation in HCC

We further analysed the effect of UBE2L3 overexpression on HCC cell proliferation. Consistently, UBE2L3 overexpression significantly facilitated cell proliferation (Figure 3A), colony formation and anchorage-independent growth of HCC cells (Figure 3B-C). Unfortunately, high expression of UBE2L3 had no significant effect on cell viability (Supplementary Figure 2). $UBE2L3^{C86S}$, a dominant-negative mutant of UBE2L3, was constructed by substituting the catalytic cysteine required for ubiquitin binding. In this part, we observed that $UBE2L3^{C86S}$ overexpression weakened the proliferation-promoting function of UBE2L3 in Huh-7 cells, indicating that the activity of ubiquitin binding enzyme is important for

UBE2L3 to regulate cell growth of HCC.

3.4 UBE2L3 influences cell proliferation and apoptosis in HCC by regulating p65 signalling

We further explored the underlying molecular mechanism of the effect of UBE2L3 on cell proliferation and apoptosis of HCC by utilizing tandem mass tag (TMT) quantitative mass spectrometry. KEGG pathway analysis showed that UBE2L3 knockout affected the apoptosis pathway-associated protein sets (Supplementary Figure 3A). Among the involved pathways, the p65-mediated pro-apoptotic pathway was found to be significantly upregulated (Supplementary Figure 3B). To validate our findings, we performed qPCR to detect the mRNA levels of target genes (PUMA, Bax, Bim, Bad and Bid) of p65 in UBE2L3 knockdown/knockout and overexpression cells. As shown in Figure 4A, the mRNA levels of the target genes in UBE2L3-deficient cells were significantly increased compared to those in the control group. In contrast, the overexpression of wild-type UBE2L3 significantly downregulated the target genes, while $UBE2L3^{C86S}$ overexpression had no effect (Figure 4A).

Nuclear factor κB (NF-κB), which consists of five family members in mammals, is involved in diverse processes, such as proliferation, apoptosis, differentiation and inflammation [17-20]. Among the homodimers or heterodimers constituted by p65 (RelA), RelB, c-Rel, NF-κB1 (p105/p50), or NF-κB2 (p100/p52), the p65-p50 heterodimer is the predominant NF-κB dimer [21]. Moreover, p65 is the primary member of NF-κB and is responsible for transcriptional activation of target genes. Since only p65 and c-Rel act as potent transcriptional activators, optimal activation of NF-κB signalling and induction of corresponding target genes depends on p65 phosphorylation and subsequent nuclear translocation [22, 23]. To further validate the effect of UBE2L3 on p65, we performed western blotting analysis to detect the protein level and phosphorylation level of p65 in both UBE2L3 knockdown/knockout and overexpression cells. Consistently, UBE2L3 depletion significantly upregulated

the protein level of p65, while UBE2L3 overexpression showed the opposite effect. Importantly, the phosphorylation level of p65 was increased in UBE2L3-depleted cells but decreased in UBE2L3-overexpressing cells (Figure 4B). UBE2L3 is a ubiquitin binding enzyme, and its enzyme activity is essential for its oncogenic function; therefore, we investigated the effect of UBE2L3 on the protein stability of p65. UBE2L3-overexpressing cells were treated with cycloheximide (CHX) to block de novo protein synthesis, and the level of p65 protein was determined by western blotting analysis. As shown in Supplementary Figure 4A, the half-life of p65 protein was not significantly decreased in UBE2L3-overexpressing cells relative to control cells, indicating that the protein stability of p65 was not influenced by UBE2L3. The results of the coimmunoprecipitation assay in our study also showed that there was no direct interaction between UBE2L3 and p65 (Supplementary Figure 4B), suggesting that UBE2L3 does not directly induce the downregulation of p65. Moreover, we also carried out experiments to investigate the activation of p65. The results of immunofluorescence analysis showed that p65 was translocated and accumulated to the nucleus in UBE2L3 knockdown cells (Figure 4C). Consistently, we found that UBE2L3 knockdown resulted in a marked redistribution of p65 to the nucleus by analysing cytoplasmic and nuclear fractions (Figure 4D). In addition, dual luciferase analysis showed that UBE2L3 knockdown enhanced the luciferase activity of NF-κB, while UBE2L3 overexpression played the opposite role (Figure 4E). As one of the downstream target genes of P65, PUMA was used as an indicator for the activation of p65 in our study. Figure 4F showed that the level of PUMA protein was increased in UBE2L3-deficient cells and decreased in UBE2L3-overexpressing cells but was not obviously changed in UBE2L3^{C86S}-overexpressing cells. Collectively, these data suggest that the anti-apoptotic activity of UBE2L3 is potentially associated with p65.

To further confirm our hypothesis, JSH-23, an inhibitor of NF-κB that inhibits NF-κB p65 nuclear translocation without affecting IκBα degradation, was used in the following study. The results showed that JSH-23 blocked the upregulation of PUMA

in UBE2L3 knockout cells (Figure 5A). Concurrently, the trypan blue exclusion assay showed that JSH-23 intervention significantly restored the proliferation ability of UBE2L3 knockout cells (Figure 5B). Importantly, we also observed that JSH-23 reduced apoptosis initiated by UBE2L3 knockout (Figure 5C). These results support the notion that UBE2L3 facilitates the cell growth and inhibits the apoptosis of HCC cells by modulating the p65 signalling pathway.

3.5 UBE2L3 depletion activates p65 by decreasing the ubiquitin-mediated proteasomal degradation of GSK3β

In a static state, the p50/p65 complex is sequestered in the inactive state by binding of NF-κB inhibitor α (IκBα) to the nuclear localization signal (NLS) of p65. The canonical pathway of p65 activation is mediated by IκBα phosphorylation and degradation [24]. Surprisingly, our data showed that UBE2L3 depletion did not influence the protein level of IκBα or the phosphorylation level of IκBα (Supplementary Figure 5A). TNF-α treatment activated the IκB kinase (IKK) complex, phosphorylated IκBα and induced IκBα degradation [25]. As a positive control, TNF-α intervention decreased the protein level of IκBα and increased the phosphorylation level of IκBα (Supplementary Figure 5A). Moreover, UBE2L3 depletion did not affect the interaction between p65 and IκBα (Supplementary Figure 5B). These results suggest that p65 activation induced by UBE2L3 depletion does not occur through the canonical NF-κB pathway.

We performed further analysis to identify other kinases known to be associated with NF-κB activation. Glycogen synthase kinase 3β (GSK3β) is reported to be involved in the regulation of NF-κB activity and p65 phosphorylation [26, 27]. Dual luciferase analysis showed that overexpression of GSK3β elevated NF-κB luciferase activity, while GSK3β knockdown did the opposite (Supplementary Figure 6A). Furthermore, GSK3β knockdown downregulated, whereas GSK3β overexpression upregulated the protein and phosphorylation levels of p65 (Supplementary Figure 6B). According to TMTs, the results showed a decreased level of GSK3β in UBE2L3

knockout cells. These data suggest that UBE2L3 deficiency-induced p65 expression and activation might depend on GSK3β.

To further explore the effect of UBE2L3 on GSK3β, we performed qPCR to detect the mRNA level of GSK3β in UBE2L3 knockdown/knockout and overexpression cells. As shown in Supplementary Figure 7, neither UBE2L3 knockdown/knockout nor overexpression affected GSK3β mRNA level. UBE2L3 depletion increased the total abundance of GSK3β and reduced the phosphorylation level (inactivated form) of GSK3β. In contrast, UBE2L3 overexpression, but not $UBE2L3^{C86S}$, decreased the total abundance of GSK3β but increased its phosphorylation level (Figure 6A). Next, we sought to determine whether UBE2L3 could influence GSK3β protein stability. The half-life of GSK3β protein was significantly decreased in UBE2L3-overexpressing cells compared to its control cells, indicating that the stability of GSK3β protein was influenced by UBE2L3 (Figure 6B). Moreover, the effect of UBE2L3 overexpression on GSK3β was blocked in the presence of the proteasome inhibitor MG132, suggesting that UBE2L3 degraded GSK3β protein via a proteasome-mediated protein degradation pathway (Figure 6C). Furthermore, a co-immunoprecipitation assay determined that endogenous and exogenous UBE2L3 were co-precipitated with endogenous and exogenous GSK3β, respectively (Figure 6D-E). Further co-immunoprecipitation assays showed that UBE2L3 depletion significantly decreased the ubiquitination of GSK3β, while UBE2L3 overexpression had the opposite effects (Figure 6F-G). Collectively, these results indicate that UBE2L3 decreases the level of GSK3β protein via ubiquitin-mediated proteasome degradation.

Next, we further investigated the regulatory role of GSK3β in the oncogenic function of UBE2L3. In this part, UBE2L3 knockout cells were treated with 1-azakenpaullone, which is a selective inhibitor of GSK3β. The results showed that both 1-azakenpaullone intervention and GSK3β inhibition blocked the upregulation of p65 and p65 phosphorylation and PUMA, which were induced by UBE2L3

knockdown (Figure 7A). Concurrently, GSK3β inhibition or treatment with 1-azakenpaullone significantly rescued UBE2L3 knockout-induced growth inhibition and apoptosis promotion in HCC cells (Figure 7B-C). Collectively, these data reveal that UBE2L3 downregulates the level of GSK3β protein via ubiquitin-mediated proteasomal degradation, consequently leading to inhibition of p65.

3.6 UBE2L3 depletion suppressed the growth of HCC in a mouse model

To further verify the oncogenic function of UBE2L3, parental cells, UBE2L3 KO cells, UBE2L3 KO cells expressing shGSK3β and UBE2L3 KO cells treated with JSH-23 were orthotopically injected into the left lobe of the liver of nude mice. Compared with the parental control group, the HCC tumour size of the UBE2L3 knockout groups was significantly decreased. Importantly, UBE2L3 knockout-induced growth inhibition was restored by GSK3β suppression or p65 inhibition (Figure 8A). Immunohistochemical analysis showed lower GSK3β and p65 levels, increased cleaved PARP levels and decreased Ki-67 levels (cell proliferation marker) in tumour tissues of UBE2L3 knockout groups. Additionally, these effects were blocked by GSK3β knockdown or p65 inhibition (Figure 8B). Altogether, these data suggest that UBE2L3 knockout in tumour tissues suppresses tumour growth and induces apoptosis *in vivo* through the GSK3β/p65 pathway.

4. Discussion

Approximately 38 genes encoding E2s are present in the human genome; these genes are classified into four classes and share a conserved domain containing the catalytic Cys residue [28]. However, the functions of E2s in cancer cells have rarely been reported. Shekhar et al. reported that UBE2B was overexpressed in the breast cell line MCF10A and potentially participated in the tumorigenesis of breast cancer [29]. Additionally, UBE2C has been reported to be overexpressed in numerous types of cancer, including lung cancer, breast cancer, bladder cancer, ovarian cancer, gastroesophageal cancer and glioblastoma. Another study demonstrated that UBE2C was associated with tumour differentiation grade and tumour development in different types of cancers [30]. Moreover, the ubiquitination and degradation of p53 and the NF-κB inhibitor IκBα were mediated by UBE2D2 and UBE2D3 [31, 32], both of which exhibit upregulated expression in breast cancer [33]. Furthermore, the level of UBE2S was also increased in breast cancer, and its high expression was involved in cell cycle regulation [34]. As for UBE2L3, its bio-function in metastatic prostate cancer and NSCLC has been previously reported [16], [15]. In the current study, we found that UBE2L3 mRNA levels were significantly higher in most HCC tissues than in the corresponding adjacent non-tumour liver tissues based on analysis of a public database. Furthermore, upregulation of UBE2L3 mRNA and protein levels was further confirmed in 90 HCC tissues vs. paired non-tumour tissues. Importantly, we observed that high expression of UBE2L3 was associated with tumour size, clinical grade and prognosis in HCC patients. The imbalance between cell proliferation and cell death plays a pivotal role in the cancer progression and development of HCC [35, 36]. Thus, we further explored the function of UBE2L3 on cell proliferation and apoptosis in HCC. UBE2L3 knockdown significantly inhibited cell proliferation and induced apoptosis, while UBE2L3 overexpression increased the proliferation of HCC cells. In a xenograft nude mouse model, we also found that knockout of UBE2L3

inhibited the progression of tumours. All the results indicated that UBE2L3 might act as an oncogene in HCC tumorigenesis.

Until now, functional studies of UBE2L3 have mainly focused on the following two aspects. One is the relationship between UBE2L3 gene polymorphisms and diseases. For example, rs140490, an alteration in the promoter region of UBE2L3, was found to be markedly associated with susceptibility to numerous autoimmune diseases, especially systemic lupus erythematosus (SLE) [37]. In addition, rs2298428, which is another alteration of UBE2L3, was demonstrated as a susceptibility factor of Crohn's disease [38]. In addition, the TCGGC haplotype of UBE2L3 was related to the increasing risk of Hashimoto's thyroiditis in the Chinese Han population [39]. UBE2L3 also regulates the protein stability of some signalling molecules, which is essential to its role in cancer regulation. Here, we demonstrated that UBE2L3 depletion inhibited cell proliferation and enhanced apoptosis in HCC cells by regulating p65. First, we confirmed that UBE2L3 depletion upregulated the expression of PUMA, Bax, Bim, Bad, and Bid, all of which are known target genes of p65. Next, we observed that UBE2L3 silencing upregulated the expression of p65 and promoted p65 protein phosphorylation and subsequent nuclear translocation, ultimately resulting in the activation of the target genes stated above. Moreover, we also revealed that JSH-23, an NF-κB p65 inhibitor, significantly restored the regulatory effect of UBE2L3 knockout on cell proliferation and apoptosis in HCC. Unfortunately, we did not observe the influence of UBE2L3 depletion on IκBα phosphorylation and degradation, which suggested that p65 activation might not be mediated by the classical signalling pathway. To our surprise, GSK3β, another previously reported regulatory factor of p65, was found to positively influence the luciferase activity of NF-κB and the expression of p65. Furthermore, we discovered the regulatory effect of UBE2L3 on the ubiquitination of GSK3β; that is, UBE2L3 depletion increased the protein stability of GSK3β and promoted its activation. Both GSK3β knockdown and treatment with 1-azakenpaullone, a GSK3β inhibitor,

significantly attenuated the effect of UBE2L3 on the proliferation and apoptosis of HCC cells, revealing a novel mechanism of UBE2L3 in regulating HCC cells through activating the GSK3β/p65 pathway. To our knowledge, although Liu et al. revealed that UBE2L3 might promote hepatocyte proliferation[40], this is the first report revealing the molecular mechanism of UBE2L3 in regulating the proliferation and apoptosis of HCC cells.

In conclusion, the present study illustrates that UBE2L3 expression is frequently upregulated in clinical HCC samples. UBE2L3 knockdown or knockout significantly inhibits the proliferation and enhances the apoptosis of HCC cells and suppresses tumour growth in mouse models. Mechanistically, we demonstrated that low expression of GSK3β in HCC cells is mediated by high level of UBE2L3 via the ubiquitin-mediated proteasome-degradation pathway, which consequently blocks p65 activation (Figure 8C). Taken together, our research proposes that UBE2L3 is a vital pro-tumorigenic factor in liver carcinogenesis.

Acknowledgements This study was supported by the National Natural Science Foundation of China (81861168035, 81871656 and 81922011, JC), Chongqing Natural Science Foundation (cstc2018jcyjAX0114, JC, cstc2019jcyj-msxmX0041, NN T and cstc2018jcyjAX0485, JH R) and Creative Research Group of CQ University (CXQT19016, JC).

Conflict of Interest Disclosure: The authors disclose no potential conflicts of interest.

Reference

[1] F. Bray, J. Ferlay, I. Soerjomataram, R.L. Siegel, L.A. Torre, A. Jemal, Global cancer statistics 2018: GLOBOCAN estimates of incidence and mortality worldwide for 36 cancers in 185 countries, CA: a cancer journal for clinicians, 68 (2018) 394-424.

[2] G. Goldstein, M. Scheid, U. Hammerling, D.H. Schlesinger, H.D. Niall, E.A.

Boyse, Isolation of a polypeptide that has lymphocyte-differentiating properties and is probably represented universally in living cells, Proc Natl Acad Sci U S A, 72 (1975) 11-15.
[3] E. Reinstein, A. Ciechanover, Narrative review: protein degradation and human diseases: the ubiquitin connection, Ann Intern Med, 145 (2006) 676-684.
[4] A. Ciechanover, Intracellular protein degradation: from a vague idea thru the lysosome and the ubiquitin-proteasome system and onto human diseases and drug targeting, Cell Death Differ, 12 (2005) 1178-1190.
[5] A.L. Goldberg, Functions of the proteasome: from protein degradation and immune surveillance to cancer therapy, Biochem Soc Trans, 35 (2007) 12-17.
[6] C.H. Liu, A.L. Goldberg, X.B. Qiu, New insights into the role of the ubiquitin-proteasome pathway in the regulation of apoptosis, Chang Gung Med J, 30 (2007) 469-479.
[7] S.I. Reed, The ubiquitin-proteasome pathway in cell cycle control, Results Probl Cell Differ, 42 (2006) 147-181.
[8] I.A. Voutsadakis, Ubiquitination and the ubiquitin - proteasome system in the pathogenesis and treatment of squamous head and neck carcinoma, Anticancer Res, 33 (2013) 3527-3541.
[9] O. Kerscher, R. Felberbaum, M. Hochstrasser, Modification of proteins by ubiquitin and ubiquitin-like proteins, Annu Rev Cell Dev Biol, 22 (2006) 159-180.
[10] P. Roos-Mattjus, L. Sistonen, The ubiquitin-proteasome pathway, Ann Med, 36 (2004) 285-295.
[11] O.D. Reyes-Hernandez, A. Mejia-Garcia, E.M. Sanchez-Ocampo, M.A. Cabanas-Cortes, P. Ramirez, L. Chavez-Gonzalez, F.J. Gonzalez, G. Elizondo, Ube2l3 gene expression is modulated by activation of the aryl hydrocarbon receptor: implications for p53 ubiquitination, Biochem Pharmacol, 80 (2010) 932-940.
[12] A. Flores-Perez, G. Elizondo, Apoptosis induction and inhibition of HeLa cell proliferation by alpha-naphthoflavone and resveratrol are aryl hydrocarbon receptor-independent, Chem Biol Interact, 281 (2018) 98-105.
[13] X. Han, L. Zhang, J. Chung, F. Mayca Pozo, A. Tran, D.D. Seachrist, J.W. Jacobberger, R.A. Keri, H. Gilmore, Y. Zhang, UbcH7 regulates 53BP1 stability and DSB repair, Proc Natl Acad Sci U S A, 111 (2014) 17456-17461.
[14] M.A. Gandini, A. Sandoval, G.W. Zamponi, R. Felix, The MAP1B-LC1/UBE2L3 complex catalyzes degradation of cell surface CaV2.2 channels, Channels (Austin), 8 (2014) 452-457.
[15] X. Ma, J. Zhao, F. Yang, H. Liu, W. Qi, Ubiquitin conjugating enzyme E2 L3 promoted tumor growth of NSCLC through accelerating p27kip1 ubiquitination and degradation, Oncotarget, 8 (2017) 84193-84203.
[16] X.S. Wang, S. Shankar, S.M. Dhanasekaran, B. Ateeq, A.T. Sasaki, X. Jing, D. Robinson, Q. Cao, J.R. Prensner, A.K. Yocum, R. Wang, D.F. Fries, B. Han, I.A. Asangani, X. Cao, Y. Li, G.S. Omenn, D. Pflueger, A. Gopalan, V.E. Reuter, E.R. Kahoud, L.C. Cantley, M.A. Rubin, N. Palanisamy, S. Varambally, A.M. Chinnaiyan,

Characterization of KRAS rearrangements in metastatic prostate cancer, Cancer Discov, 1 (2011) 35-43.
[17] E. Jacque, K. Billot, H. Authier, D. Bordereaux, V. Baud, RelB inhibits cell proliferation and tumor growth through p53 transcriptional activation, Oncogene, 32 (2013) 2661-2669.
[18] E. Pazarentzos, A.L. Mahul-Mellier, C. Datler, W. Chaisaklert, M.S. Hwang, J. Kroon, D. Qize, F. Osborne, A. Al-Rubaish, A. Al-Ali, N.D. Mazarakis, E.O. Aboagye, S. Grimm, IkappaBetaalpha inhibits apoptosis at the outer mitochondrial membrane independently of NF-kappaB retention, Embo j, 33 (2014) 2814-2828.
[19] J. Jin, H. Hu, H.S. Li, J. Yu, Y. Xiao, G.C. Brittain, Q. Zou, X. Cheng, F.A. Mallette, S.S. Watowich, S.C. Sun, Noncanonical NF-kappaB pathway controls the production of type I interferons in antiviral innate immunity, Immunity, 40 (2014) 342-354.
[20] J.A. DiDonato, F. Mercurio, M. Karin, NF-kappaB and the link between inflammation and cancer, Immunol Rev, 246 (2012) 379-400.
[21] R. Moreno, J.M. Sobotzik, C. Schultz, M.L. Schmitz, Specification of the NF-kappaB transcriptional response by p65 phosphorylation and TNF-induced nuclear translocation of IKK epsilon, Nucleic Acids Res, 38 (2010) 6029-6044.
[22] G. Fiume, E. Vecchio, A. De Laurentiis, F. Trimboli, C. Palmieri, A. Pisano, C. Falcone, M. Pontoriero, A. Rossi, A. Scialdone, F. Fasanella Masci, G. Scala, I. Quinto, Human immunodeficiency virus-1 Tat activates NF-kappaB via physical interaction with IkappaB-alpha and p65, Nucleic Acids Res, 40 (2012) 3548-3562.
[23] H. Takeuchi, T. Hirano, S.E. Whitmore, I. Morisaki, A. Amano, R.J. Lamont, The serine phosphatase SerB of Porphyromonas gingivalis suppresses IL-8 production by dephosphorylation of NF-kappaB RelA/p65, PLoS Pathog, 9 (2013) e1003326.
[24] S.M. Evans, K.G. Rodino, Orientia tsutsugamushi uses two Ank effectors to modulate NF-kappaB p65 nuclear transport and inhibit NF-kappaB transcriptional activation, 14 (2018) e1007023.
[25] T. Tanaka, M. Iino, Nuclear Translocation of p65 is Controlled by Sec6 via the Degradation of IkappaBalpha, J Cell Physiol, 231 (2016) 719-730.
[26] S. Kotliarova, S. Pastorino, L.C. Kovell, Y. Kotliarov, H. Song, W. Zhang, R. Bailey, D. Maric, J.C. Zenklusen, J. Lee, H.A. Fine, Glycogen synthase kinase-3 inhibition induces glioma cell death through c-MYC, nuclear factor-kappaB, and glucose regulation, Cancer Res, 68 (2008) 6643-6651.
[27] C. Dudgeon, R. Peng, P. Wang, A. Sebastiani, J. Yu, L. Zhang, Inhibiting oncogenic signaling by sorafenib activates PUMA via GSK3beta and NF-kappaB to suppress tumor cell growth, Oncogene, 31 (2012) 4848-4858.
[28] C. Xie, C. Powell, M. Yao, J. Wu, Q. Dong, Ubiquitin-conjugating enzyme E2C: a potential cancer biomarker, Int J Biochem Cell Biol, 47 (2014) 113-117.
[29] M.P. Shekhar, B. Gerard, R.J. Pauley, B.O. Williams, L. Tait, Rad6B is a positive regulator of beta-catenin stabilization, Cancer Res, 68 (2008) 1741-1750.
[30] K.W. Wagner, L.M. Sapinoso, W. El-Rifai, H.F. Frierson, N. Butz, J. Mestan, F.

Hofmann, Q.L. Deveraux, G.M. Hampton, Overexpression, genomic amplification and therapeutic potential of inhibiting the UbcH10 ubiquitin conjugase in human carcinomas of diverse anatomic origin, Oncogene, 23 (2004) 6621-6629.
[31] M.K. Saville, A. Sparks, D.P. Xirodimas, J. Wardrop, L.F. Stevenson, J.C. Bourdon, Y.L. Woods, D.P. Lane, Regulation of p53 by the ubiquitin-conjugating enzymes UbcH5B/C in vivo, J Biol Chem, 279 (2004) 42169-42181.
[32] H. Gonen, B. Bercovich, A. Orian, A. Carrano, C. Takizawa, K. Yamanaka, M. Pagano, K. Iwai, A. Ciechanover, Identification of the ubiquitin carrier proteins, E2s, involved in signal-induced conjugation and subsequent degradation of IkappaBalpha, J Biol Chem, 274 (1999) 14823-14830.
[33] L. Chen, K. Madura, Increased proteasome activity, ubiquitin-conjugating enzymes, and eEF1A translation factor detected in breast cancer tissue, Cancer Res, 65 (2005) 5599-5606.
[34] D. Tedesco, J. Zhang, L. Trinh, G. Lalehzadeh, R. Meisner, K.D. Yamaguchi, D.L. Ruderman, H. Dinter, D.A. Zajchowski, The ubiquitin-conjugating enzyme E2-EPF is overexpressed in primary breast cancer and modulates sensitivity to topoisomerase II inhibition, Neoplasia, 9 (2007) 601-613.
[35] H. Ehedego, A. Mohs, B. Jansen, K. Hiththetiya, P. Sicinski, C. Liedtke, C. Trautwein, Loss of Cyclin E1 attenuates hepatitis and hepatocarcinogenesis in a mouse model of chronic liver injury, Oncogene, (2018).
[36] J.J. Liu, Y. Li, W.S. Chen, Y. Liang, G. Wang, M. Zong, K. Kaneko, R. Xu, M. Karin, G.S. Feng, Shp2 deletion in hepatocytes suppresses hepatocarcinogenesis driven by oncogenic beta-Catenin, PIK3CA and MET, J Hepatol, (2018).
[37] M.J. Lewis, S. Vyse, A.M. Shields, S. Boeltz, P.A. Gordon, T.D. Spector, P.J. Lehner, H. Walczak, T.J. Vyse, UBE2L3 polymorphism amplifies NF-kappaB activation and promotes plasma cell development, linking linear ubiquitination to multiple autoimmune diseases, Am J Hum Genet, 96 (2015) 221-234.
[38] K. Fransen, M.C. Visschedijk, S. van Sommeren, J.Y. Fu, L. Franke, E.A. Festen, P.C. Stokkers, A.A. van Bodegraven, J.B. Crusius, D.W. Hommes, P. Zanen, D.J. de Jong, C. Wijmenga, C.C. van Diemen, R.K. Weersma, Analysis of SNPs with an effect on gene expression identifies UBE2L3 and BCL3 as potential new risk genes for Crohn's disease, Hum Mol Genet, 19 (2010) 3482-3488.
[39] Y. Wang, Y.F. Zhu, Q. Wang, J. Xu, N. Yan, J. Xu, L.F. Shi, S.T. He, J.A. Zhang, The haplotype of UBE2L3 gene is associated with Hashimoto's thyroiditis in a Chinese Han population, BMC Endocr Disord, 16 (2016) 18.
[40] Y. Liu, C. Song, H. Ni, W. Jiao, W. Gan, X. Dong, J. Liu, L. Zhu, X. Zhai, Z. Hu, J. Li, UBE2L3, a susceptibility gene that plays oncogenic role in hepatitis B-related hepatocellular carcinoma, Journal of viral hepatitis, 25 (2018) 1363-1371.

Table 1. Correlative analysis of UBE2L3 protein levels with clinicopathologic features.

Clinicopatholigic Parameters	No.of Specimens	UBE2L3 Expression (Tumor / Non-tumor) High(>1)	Low(<1)	P Value
Sex	90			0.718
Female	13	9	4	
Male	77	57	20	
Age	90			0.924
≤50	42	31	11	
>50	48	35	13	
ALT	90			0.868
≤40 u/l	45	32	13	
40-100 u/l	40	30	10	
≥100 u/l	5	4	1	
AST	90			0.823
≤40 u/l	42	32	10	
40-100 u/l	42	30	12	
≥100 u/l	6	4	2	
AFP	90			0.318
≤20 ng/ml	39	26	13	
20-300 ng/ml	31	23	8	
≥300 ng/ml	20	17	3	
Tumor size	90			0.007
≤3 cm	19	11	8	
3-5 cm	17	9	8	
≥5 cm	54	46	8	
Tumor number	90			0.861
=1	76	56	20	
>1	14	10	4	
Grade	90			0.011
1	12	6	6	
2	51	35	16	
3	27	25	2	
Vascular invasion	90			0.771
No	56	43	13	
Yes	34	27	7	
Cirrhosis	90			0.646
No	34	24	10	
Yes	56	42	14	
HBV	90			0.800
No	10	7	3	
Yes	80	59	21	

Figure 1

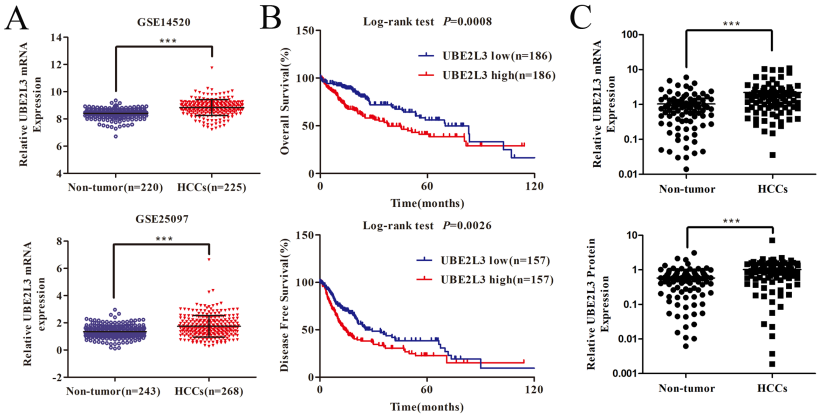
A
GSE14520
***
Relative UBE2L3 mRNA Expression
Non-tumor(n=220)
HCCs(n=225)
GSE25097
***
Relative UBE2L3 mRNA expression
Non-tumor(n=243)
HCCs(n=268)
B
Log-rank test P=0.0008
UBE2L3 low(n=186)
UBE2L3 high(n=186)
Overall Survival(%)
Time(months)
Log-rank test P=0.0026
UBE2L3 low(n=157)
UBE2L3 high(n=157)
Disease Free Survival(%)
Time(months)
C
***
Relative UBE2L3 mRNA Expression
Non-tumor
HCCs
***
Relative UBE2L3 Protein Expression
Non-tumor
HCCs

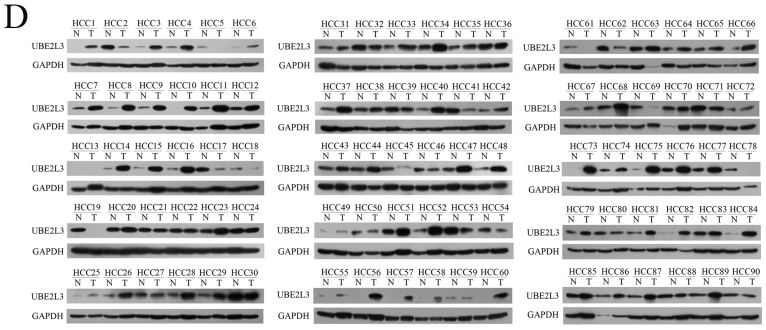
D
UBE2L3
GAPDH

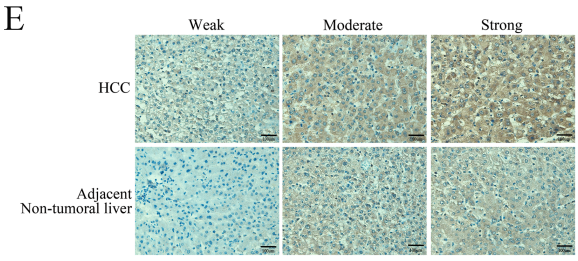
E
Weak
Moderate
Strong
HCC
Adjacent Non-tumoral liver

Figure 2

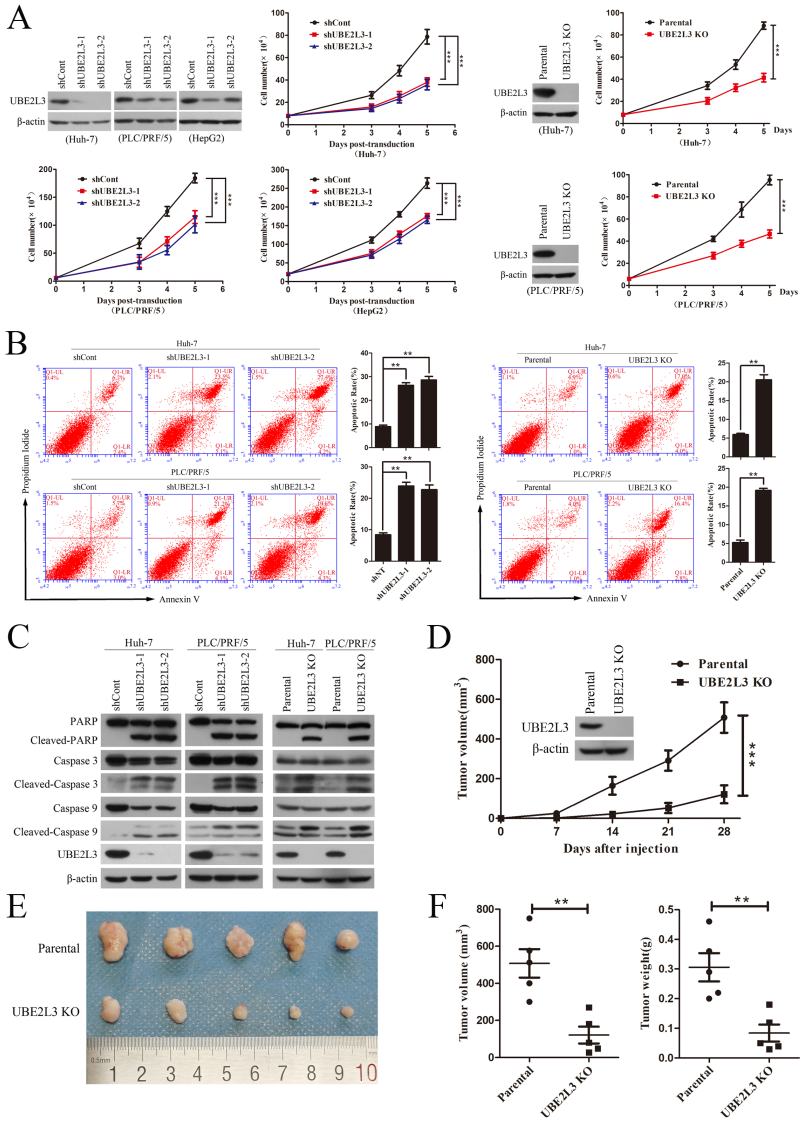
A
shCont
shUBE2L3-1
shUBE2L3-2
UBE2L3
β-actin
(Huh-7)
(PLC/PRF/5)
(HepG2)
Cell number(×10⁴)
Days post-transduction
(Huh-7)
(PLC/PRF/5)
(HepG2)
Parental
UBE2L3 KO
Days
B
Huh-7
PLC/PRF/5
Propidium Iodide
Annexin V
Apoptotic Rate(%)
C
PARP
Cleaved-PARP
Caspase 3
Cleaved-Caspase 3
Caspase 9
Cleaved-Caspase 9
D
Tumor volume(mm³)
Days after injection
E
F
Tumor volume (mm³)
Tumor weight(g)

Figure 3

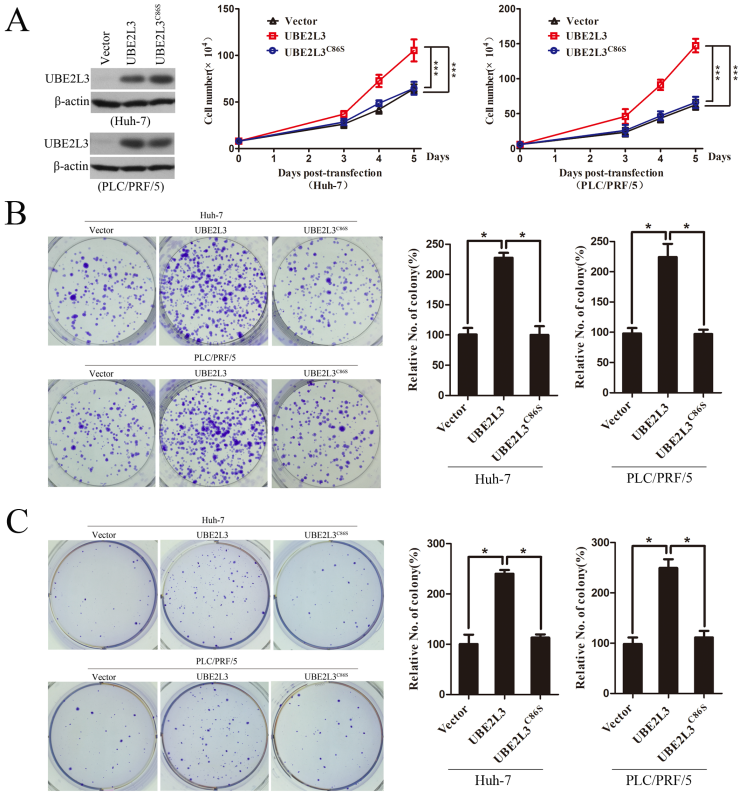
A
Vector
UBE2L3
UBE2L3C86S
UBE2L3
β-actin
(Huh-7)
UBE2L3
β-actin
(PLC/PRF/5)
Cell number(× 10⁴)
Days post-transfection
(Huh-7)
(PLC/PRF/5)
Days
B
Huh-7
PLC/PRF/5
Relative No. of colony(%)
C

Figure 4

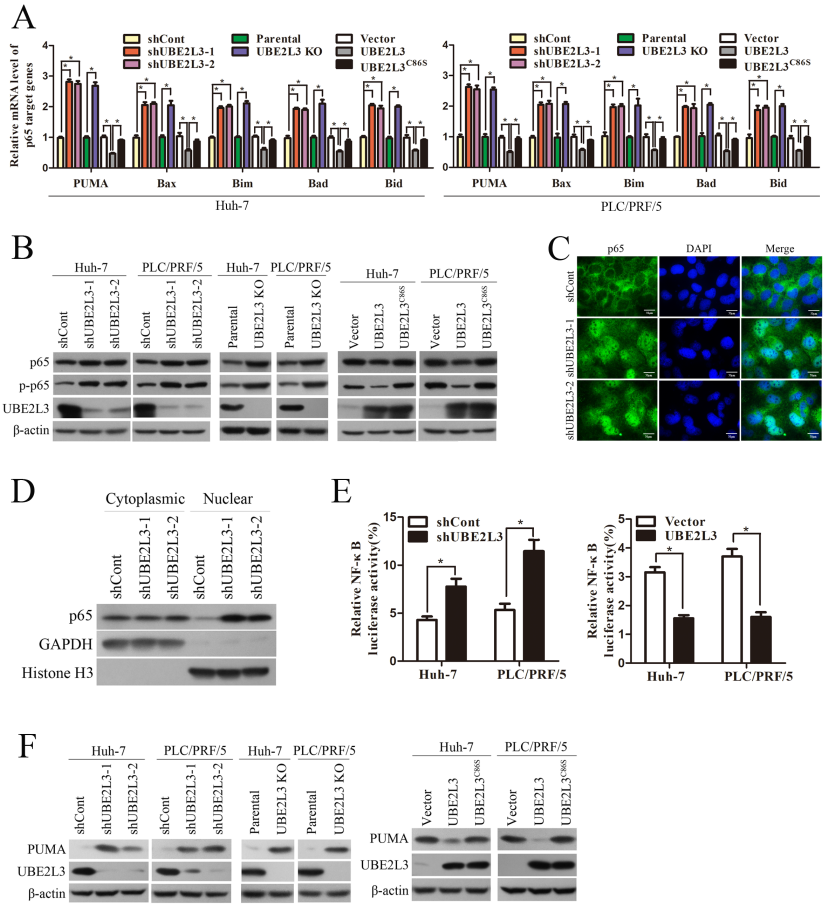
A
shCont
shUBE2L3-1
shUBE2L3-2
Parental
UBE2L3 KO
Vector
UBE2L3
UBE2L3C86S
Relative mRNA level of p65 target genes
PUMA
Bax
Bim
Bad
Bid
Huh-7
PLC/PRF/5
B
Huh-7
PLC/PRF/5
p65
p-p65
UBE2L3
β-actin
C
p65
DAPI
Merge
shCont
shUBE2L3-1
shUBE2L3-2
D
Cytoplasmic
Nuclear
GAPDH
Histone H3
E
Relative NF-κ B luciferase activity(%)
F
PUMA
UBE2L3
β-actin

Figure 5

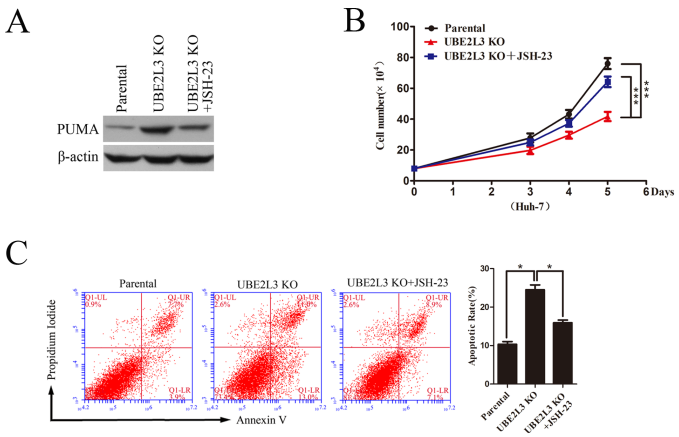
A
Parental
UBE2L3 KO
UBE2L3 KO +JSH-23
PUMA
β-actin
B
Parental
UBE2L3 KO
UBE2L3 KO＋JSH-23
Cell number(× 10⁴)
Days
(Huh-7)
***
***
C
Parental
UBE2L3 KO
UBE2L3 KO+JSH-23
Propidium Iodide
Annexin V
Apoptotic Rate(%)
*
*

Figure 6

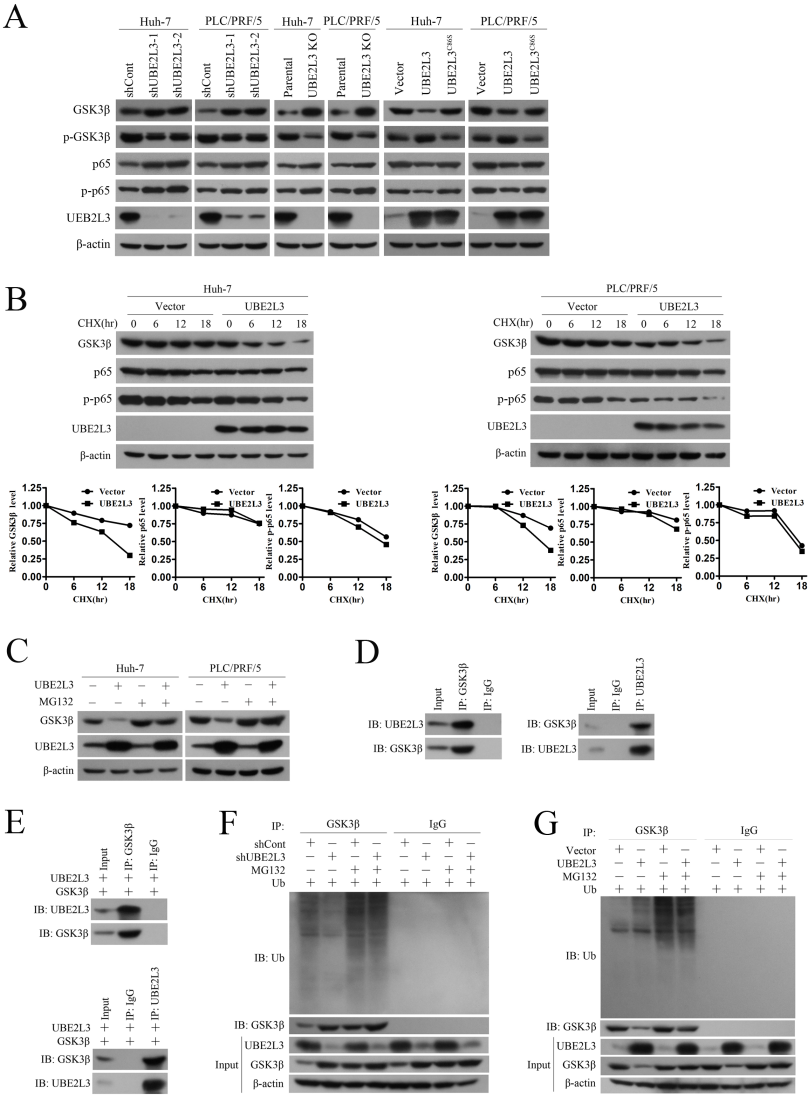
A
Huh-7
PLC/PRF/5
Huh-7
PLC/PRF/5
Huh-7
PLC/PRF/5
shCont
shUBE2L3-1
shUBE2L3-2
shCont
shUBE2L3-1
shUBE2L3-2
Parental
UBE2L3 KO
Parental
UBE2L3 KO
Vector
UBE2L3
UBE2L3C93S
Vector
UBE2L3
UBE2L3C93S
GSK3β
p-GSK3β
p65
p-p65
UEB2L3
β-actin
B
Huh-7
PLC/PRF/5
Vector
UBE2L3
CHX(hr) 0 6 12 18 0 6 12 18
GSK3β
p65
p-p65
UBE2L3
β-actin
Relative GSK3β level
Relative p65 level
Relative p-p65 level
CHX(hr)
C
Huh-7
PLC/PRF/5
UBE2L3
MG132
GSK3β
UBE2L3
β-actin
D
Input
IP: GSK3β
IP: IgG
IB: UBE2L3
IB: GSK3β
Input
IP: IgG
IP: UBE2L3
IB: GSK3β
IB: UBE2L3
E
Input
IP: GSK3β
IP: IgG
UBE2L3
GSK3β
IB: UBE2L3
IB: GSK3β
Input
IP: IgG
IP: UBE2L3
UBE2L3
GSK3β
IB: GSK3β
IB: UBE2L3
F
IP:
GSK3β
IgG
shCont
shUBE2L3
MG132
Ub
IB: Ub
IB: GSK3β
Input
UBE2L3
GSK3β
β-actin
G
IP:
GSK3β
IgG
Vector
UBE2L3
MG132
Ub
IB: Ub
IB: GSK3β
Input
UBE2L3
GSK3β
β-actin

Figure 7

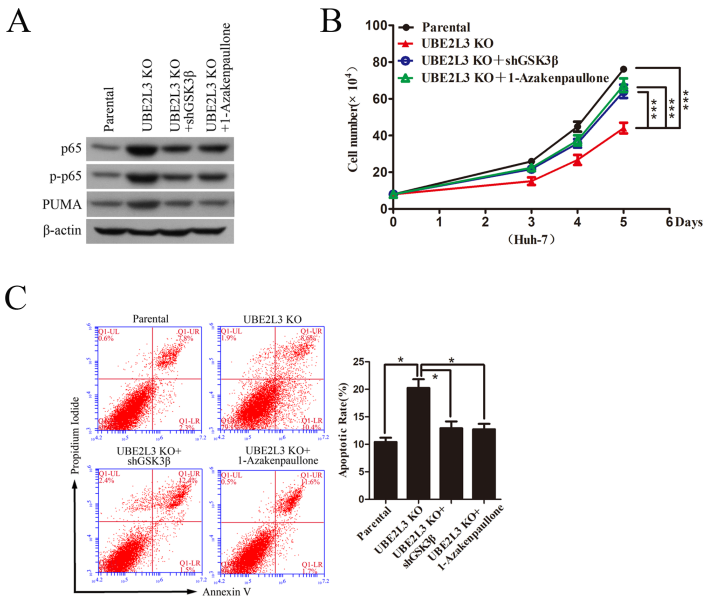
A
Parental
UBE2L3 KO
UBE2L3 KO +shGSK3β
UBE2L3 KO +1-Azakenpaullone
p65
p-p65
PUMA
β-actin
B
Parental
UBE2L3 KO
UBE2L3 KO＋shGSK3β
UBE2L3 KO＋1-Azakenpaullone
Cell number(× 10⁴)
Days
(Huh-7)
C
Parental
UBE2L3 KO
UBE2L3 KO+ shGSK3β
UBE2L3 KO+ 1-Azakenpaullone
Propidium Iodide
Annexin V
Apoptotic Rate(%)

Figure 8

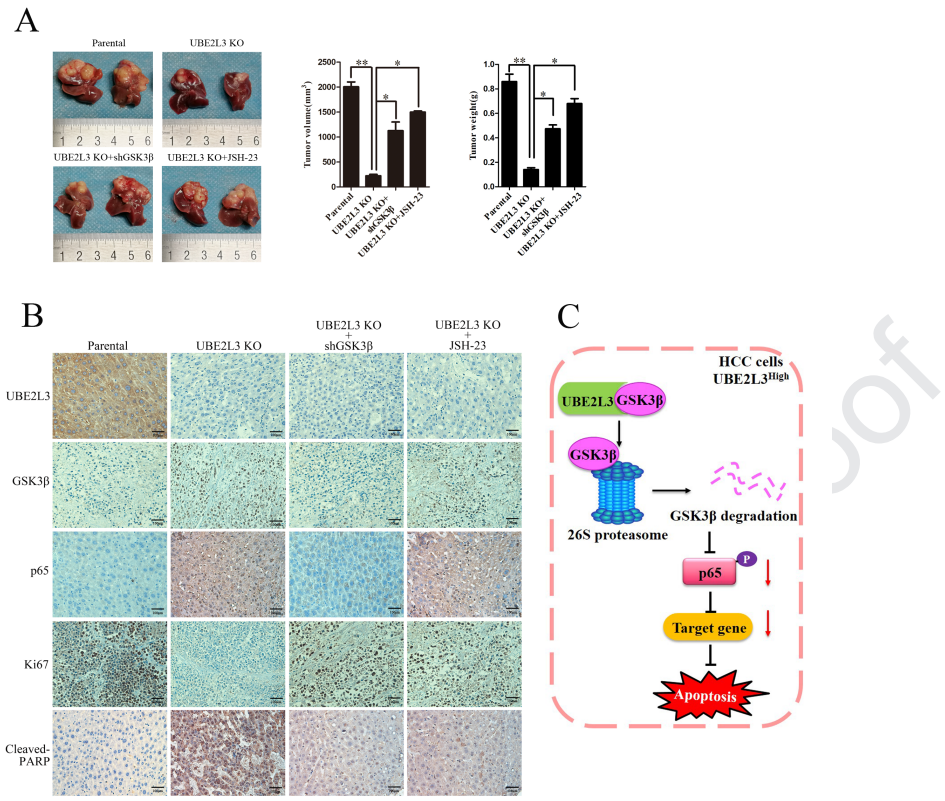
A
Parental
UBE2L3 KO
UBE2L3 KO+shGSK3β
UBE2L3 KO+JSH-23
Tumor volume(mm³)
Tumor weight(g)
Parental
UBE2L3 KO
UBE2L3 KO+ shGSK3β
UBE2L3 KO+JSH-23
B
Parental
UBE2L3 KO
UBE2L3 KO + shGSK3β
UBE2L3 KO + JSH-23
UBE2L3
GSK3β
p65
Ki67
Cleaved-PARP
C
HCC cells
UBE2L3High
UBE2L3
GSK3β
GSK3β
26S proteasome
GSK3β degradation
p65
P
Target gene
Apoptosis

Figure 1. Expression of UBE2L3 is upregulated in HCC tissues and correlates with survival of patients with HCC

(A) The mRNA levels of UBE2L3 in adjacent non-tumour tissues (Non-tumour) and HCC tissues (HCCs) were illustrated by scatterplot. GEO database: GSE14520, GSE25097. ***P < 0.001. (B) Kaplan-Meier analysis of the correlation between UBE2L3 level and survival in the TCGA cohort. The correlation between UBE2L3 level and overall survival. P=0.0008. The correlation between UBE2L3 level and diseases free survival. P=0.0026. (C) The mRNA levels of UBE2L3 in Non-tumour group and in HCCs group were tested by RT-qPCR. β-actin mRNA level was used as an internal control. ***P < 0.001. The statistical graph of UBE2L3 protein levels in Non-tumour group v.s in HCCs group. ***P < 0.001. (D) The protein expression levels of UBE2L3 in Non-tumour group and in HCCs group were analysed by western blotting analysis. GAPDH was used as a loading control. (E) IHC staining of HCC tissues and their adjacent non-tumoural liver tissues. Magnification, × 400.

Figure 2. UBE2L3 deficiency inhibits proliferation and tumourigenesis of HCC *in vitro* and *in vivo*

(A) The efficiency of UBE2L3 knockdown or knockout in HCC cells was detected by western blotting analysis. β-actin was used as a loading control. The effect of UBE2L3 knockdown or knockout on the proliferation of HCC cells were analysed by typan blue exclusion assays. ***P < 0.001. (B) The effect of UBE2L3 knockdown or knockout on the apoptosis of HCC cells were assayed by Flow Cytometry. **P < 0.01. (C) The effect of UBE2L3 knockdown or knockout on the apoptosis-related factors expression level in HCC cells were analysed by western blotting analysis. β-actin was used as a loading control. (D) The growth curve of the xenografted tumour of UBE2L3 KO cells and its parental cells. ***P < 0.001. The efficiency of UBE2L3 knockout in HCC cells was detected by western blotting analysis. β-actin was used as a loading control. (E) The picture of the xenografted tumour of UBE2L3 KO cells and its parental cells. (F) The volume and weight statistical graph of the xenografted

tumour of UBE2L3 KO cells and its parental cells. $^{**}P < 0.01$.

Figure 3. UBE2L3 overexpression promotes HCC cell proliferation

(A) The efficiency of UBE2L3 overexpression in HCC cells was detected by western blotting analysis. β-actin was used as a loading control. The effect of UBE2L3 overexpression on the proliferation of HCC cells was analysed by typan blue exclusion assays. $^{***}P < 0.001$. (B) The effect of UBE2L3 overexpression on the ability of colony formation in HCC cells was detected by colony formation assays. $^{*}P < 0.05$. (C) The effect of UBE2L3 overexpression on the ability of anchorage-dependent growth in HCC cells was detected by soft agar assays. $^{*}P < 0.05$.

Figure 4. UBE2L3 influences HCC cell proliferation and apoptosis by regulating p65 signaling

(A) The effect of UBE2L3 knockdown, knockout or overexpression on the mRNA expression levels of p65 target genes were tested by RT-qPCR. β-actin mRNA expression was used as an internal control. $^{*}P < 0.05$. (B) The effect of UBE2L3 knockdown, knockout or overexpression on the protein expression level and phosphorylation level of p65 were analysed by western blotting analysis. β-actin was used as a loading control. (C) The protein expression level and subcellular location of p65 in the UBE2L3 knock down cells were detected by ICC. Immunofluorescence analysis of DAPI (blue) and p65 (green) showed that depleted UBE2L3 promoted the expression and nuclear translocation of p65. (D) The cytoplasmic and nuclear protein in UBE2L3 knock down cells were extracted and used for the detection of p65 protein expression level and subcellular location. GAPDH and Histone H3 were used as markers for the cytoplasmic and nuclear fractions, respectively. (E) The transcriptional activity of NF-κB was detected by dual-luciferase reporter assay. The influence of UBE2L3 knock down and UBE2L3 overexpression on transcriptional activity of NF-κB. $^{*}P < 0.05$. (F) The effect of UBE2L3 knockdown, knockout or

overexpression on the protein expression level of PUMA were analysed by western blotting analysis. β-actin was used as a loading control.

Figure 5. p65 inhibitor JSH-23 reverses the effect of UBE2L3 deficiency

(A) The effect of p65 inhibitor JSH-23 on the UBE2L3 downstream signaling pathway was analysed by western blotting analysis. (B) The reverse effect of p65 inhibitor JSH-23 on the UBE2L3 KO-induced proliferation inhibition was analysed by typan blue exclusion assays. ***$P < 0.001$. (C) The reverse effect of JSH-23 on the UBE2L3 KO-induced apoptosis were assayed by Flow Cytometry. *$P < 0.05$.

Figure 6. UBE2L3 deficiency activates p65 by decreasing the ubiquitin-mediated proteasome degradation of GSK3β

(A) The effect of UBE2L3 knockdown, knockout or overexpression on the protein expression level and phosphorylation level of GSK3β were analysed by western blotting analysis. β-actin was used as a loading control. (B) The effect of UBE2L3 on the protein stability of GSK3β was determined by western blotting analysis. Cells were treated with 10μmol/L CHX for 0, 6, 12, 18 hours. β-actin was used as a loading control. Take the blot band gray value of 0h as 1, compared and drew the curve graph. (C) Whether UBE2L3 regulated GSK3β protein degradation through the ubiquitin-proteasome degradation pathway was determined by western blotting analysis. Cells were treated with 10μmol/L MG132 for 12 hours. β-actin was used as a loading control. (D) The association between endogenous UBE2L3 and GSK3β was measured by Co-IP. IP was conducted with Huh-7 cell lysates by using anti-GSK3β and anti-IgG antibodies or anti-UBE2L3 and anti-IgG antibodies, and IB was performed with anti-UBE2L3 and anti-GSK3β antibodies or anti-GSK3β and anti-UBE2L3 antibodies. (E) The association between exogenous UBE2L3 and GSK3β was measured by Co-IP. IP was conducted with Huh-7 cell lysates that were prepared from UBE2L3 and GSK3β overexpression cells by using anti-GSK3β and anti-IgG antibodies or anti-UBE2L3 and anti-IgG antibodies, and IB was performed

with anti-UBE2L3 and anti-GSK3β antibodies or anti-GSK3β and anti-UBE2L3 antibodies. (F) The effect of UBE2L3 on the ubiquitination level of GSK3β was analysed by Co-IP. IP was conducted with Huh-7 cell lysates that were prepared from UBE2L3 knock down cells by using anti-GSK3β and anti-IgG antibodies, and IB was performed with anti-Ub and anti-GSK3β antibodies. (G) IP was conducted with Huh-7 cell lysates that were prepared from UBE2L3 overexpression cells by using anti-GSK3β and anti-IgG antibodies, and IB was performed with anti-Ub and anti-GSK3β antibodies.

Figure 7. GSK3β inhibitor 1-Azakenpaullone reverses the effect induced by UBE2L3 deficiency

(A) The effect of GSK3β knockdown or GSK3β inhibitor 1-azakenpaullone on the UBE2L3 downstream signaling pathway were analysed by western blotting analysis. (B) The effect of GSK3β knockdown or GSK3β inhibitor 1-azakenpaullone on the reverse of UBE2L3 KO decreased cells proliferation were analysed by typan blue exclusion assays. ***$P < 0.001$. (C) The reverse effect of GSK3β knockdown or GSK3β inhibitor 1-azakenpaullone on UBE2L3 KO-induced apoptosis were assayed by Flow Cytometry. *$P < 0.05$.

Figure 8. UBE2L3 deficiency suppresses tumour growth in orthotopic HCC nude mouse models

(A) The effect of UBE2L3 KO and GSK3β knockdown or p65 inhibitor JSH-23 on tumour growth in orthotopic xenograft model. The picture of the orthotopic tumour of UBE2L3 KO cells and GSK3β knockdown or p65 inhibitor JSH-23 treatment, and its parental cells. Near it was the volume statistical graph of the xenograft tumours. *$P <$ 0.05, **$P < 0.01$. (B) Representative images of IHC staining of UBE2L3, GSK3β, p65, Ki67 and cleaved-PARP in tumour orthotopic xenografts. Magnification, × 400. (C) The summary of how UBE2L3 promotes HCC cells proliferation through GSK3β/p65 pathway.

Highlights

- We found that UBE2L3 was frequently up-regulated in clinical HCC samples, which was associated with poor prognosis.
- UBE2L3 depletion inhibited cell proliferation and promoted cell apoptosis by through promoting GSK3β/p65 pathway in vitro and in vivo.
- UBE2L3 overexpression decreased the protein stability of GSK3β via ubiquitin-mediated proteasome degradation.